Seismic Performance of Large-Scale Reinforced Concrete Columns with Different Shear-Span Ratios

DOI: 10.23977/jceup.2025.070218 ISSN 2616-3969 Vol. 7 Num. 2

Yao Liu

China Railway Tunnel Group Special High-Tech Co., Ltd., 201306, Shanghai, China tintin0918@outlook.com

Keywords: Large-Scale Specimen, Reinforced Concrete Columns, Seismic Behavior, Bending Failure, Shear Bond Failure

Abstract: Two large-scale reinforced concrete column specimens were designed to investigate seismic performance, one for bending failure and the other for shear bond failure. Tested under low cycle reversed loading using a 40000kN loading system, the specimens' seismic behavior was analyzed in terms of failure characteristics, hysteretic behavior, deformation, and energy dissipation. Results indicate that specimen WF-4-7-.4 exhibited bending failure, demonstrating superior energy dissipation and deformation capacity with the plastic hinge region accounting for approximately 90% of total deformation. In contrast, specimen JF-2-7-.4 experienced shear bond failure, displaying narrow hysteresis curves, low energy dissipation capacity, and reduced ductility.

1. Introduction

With urban development, the construction of high-rise buildings has increased, leading to larger reinforced concrete columns. Previous studies on the seismic performance of reinforced concrete columns primarily involved small-scale specimens due to testing constraints [1-4], limiting the examination of large-scale specimens, particularly those with high axial pressure ratios. HE et al. [5] conducted tests on two sets of specimens to investigate the impact of confining steel bars on the failure modes of reinforced concrete columns with a cross-section size of 700 mm and an axial compression ratio of .05. XIAO [6] and LV [7] tested reinforced concrete columns with high axial compression ratios and cross-section sizes of 510 mm × 510 mm and 450 mm × 650 mm, respectively, focusing on high-strength concrete. Notably, SONG et al. [8] tested large-scale columns under axial compression, with the largest cross-section size being 800 mm, revealing distinct axial compression behaviors between large-scale and small-scale specimens. Furthermore, various studies [9-14] have demonstrated a decrease in compressive strength with increasing section size. However, SHAMIM and MURAT [15] observed a reduction in post-peak ductility with increasing specimen size in their study on short columns.

The seismic performance of large-scale columns under high axial compression ratios has not been thoroughly investigated. This study aims to elucidate the seismic behavior of specimens experiencing various failure modes, such as bending and shear failures, through experiments involving two specimens subjected to low-cycle reversed loading. The specimens were designed with varying shear-span ratios and volumetric ratios of transverse reinforcement. The investigation

focused on their seismic characteristics, encompassing failure modes, hysteretic behavior, deformations, and energy dissipation.

2. Experimental design

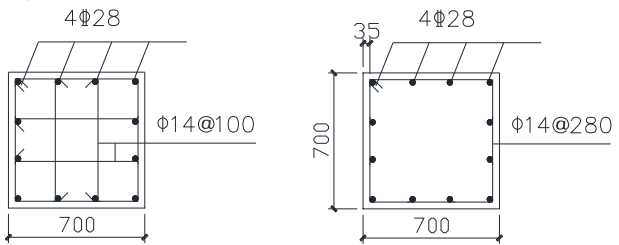
2.1 Specimens and mechanical properties of materials

The cross-sectional dimensions of two specimens were both 700 mm \times 700 mm. The volumetric ratio of transverse reinforcement (ρ_v) was 1.89% and 0.338% for the respective specimens, while the shear span ratios (λ) were 4.39 and 2.39. The experimental axial compression ratio (n) was 0.4, with the concrete grade being C30. The longitudinal steel bars were of grade HRB400 with a yield strength of 422 MPa, while the transverse reinforcement was of grade HPB300 with a yield strength of 327 MPa. Specific details of the specimens can be found in Table 1, and the section sizes and steel bar configurations are illustrated in Figure 1.

H/ $b \times h/$ f_{cp}/ c/ N/ transverse longitudinal $\rho_v/\%$ Number mm^2 mm **MPa** mm kN reinforced steel bar WF-4-7-0.4 700×700 2548 + 2504.39 0.4 4\phi14@100 1.89 30 35 5880 12**⊉**28 JF-2-7-0.4 700×700 1274+250 30 2.39 0.4 5880 2\phi14@280 12028 0.338 35

Table 1 Details of specimens

Notes: b and h are the width and height of cross-section; The letter F is low cycle reversed loading; N is axial loading; f_{cp} is the compressive strength of concrete cubic (150 mm \times 150 mm); actual shear span ratio λ =H/h₀, H is the height of specimen, the value in front of the plus is the height of the column, the value behind the plus is the height of the joint(fig.2). c is the thickness of concrete cover.



(a) First group (b) Second group

Fig.1 Section size and steel bar of specimens

2.2 Test method and test content

2.2.1 Setup of experiment

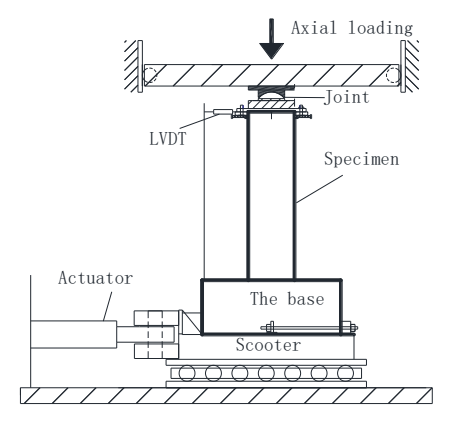


Fig.2 Test set-up

The 40000 kN multiple function electro hydraulic servo test machine (see Fig. 2) was used to apply monotonic horizontal loading and low cycle reversed loading. The axial loading was applied to the top of the joint, which was connected to the steel beam, and the lower part was connected to the specimen to ensure that the specimen only rotation without horizontal displacement at the top. The height of joint was 250mm. The base and the equipment scooter were connected to the horizontal motion.

Before the yield status of specimen was reached, the force control method was applied in the loading process. Then, after the yield status of specimen, the displacement control method was applied until the specimen failed.

2.2.2 Deformation measure

The specimens were instrumented with linear variable differential transformers (LVDT) to measure horizontal deformations, as shown in Fig. 3, The scale range of LVDT was 300 mm. In order to ensure that the measured displacement was the horizontal deformation, the bar that connect LVDT was fixed with the base, the load-displacement curves of specimen were obtained. In addition, 10 dial indicators were installed at the bottom of the column to measure bending deformation, shear deformation and bonding slip deformation of the plastic hinge region, as shown in Fig.3.

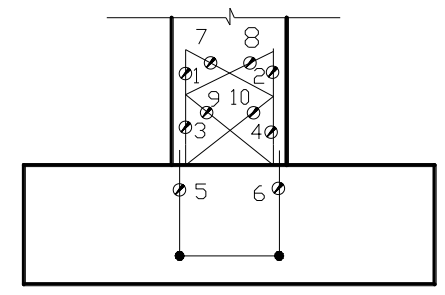


Fig.3 Installation position of dial indicators

3. Test results and analysis of the first group specimens

3.1 Failure modes

When the horizontal load is applied to 2 times yield displacement, the compressive zone of specimen WF-4-7-0.4 has a long vertical crack, which is about 400mm in length. When the horizontal load is applied to 3 times yield displacement, there are no new level cracks, 6~7 horizontal cracks were found within the range of 1.5h highly, however, there are more and more vertical cracks in the compression zone. Then the horizontal cracks of above 0.5 h are developed along the horizontal direction, and then it goes down the slope, the angle is about 45 °. When 5 times yield displacement is applied on the specimens, the concrete protection layer in the pressure area of specimen is falling down, and the longitudinal bars are bent by compression. So the specimens occur bend failure, the features of final failure pattern are shown in Fig.4(a).

When the load is 750kN, a vertical crack is found in the middle of specimen JF-2-7-0.4, and extends down from the top of specimen When the horizontal load is applied to -900kN, two horizontal cracks appear in the left of specimen, which the distance to the base of specimen are 100mm and 200mm, respectively. At 900kN, a horizontal crack in the right root was about 110mm. when the horizontal displacement applied to 4 mm (Δ =4mm), there is no new crack appeared, but the horizontal crack widening and extends along the horizontal direction, and vertical cracks continue to down, two horizontal cracks of about 200mm appear in the right of specimen, which the

distance to the base of specimen are 180mm and 350mm, respectively. When the horizontal displacement applied to 6 mm (Δ =6mm), a 200mm vertical crack appear in the left of specimen, and many of the diagonal cracks appear next to the initial vertical cracks. When the horizontal displacement is applied to 10mm, the vertical cracks are widened, and there are more diagonal cracks in the area around it, and the concrete is falling off. When the horizontal displacement is applied to 14mm, large area concrete quickly falls off, the specimen failure, as shown in Fig.4(b).



(a) WF-4-7-0.4 (b) JF-2-7-0.6

Fig.4 Final failure states of specimens

3.2 Load-displacement curve of specimens

The load-displacement curves of specimens are shown in Fig.5. It can be seen from the curve, the hysteresis curves of the specimen WF-4-7-0.4 is full, however, the hysteresis curve of the specimen JF-2-7-0.4 is narrow, after the peak load, the bearing capacity of the specimen fall fast and the deformation is smaller, so it has a poor ductility.

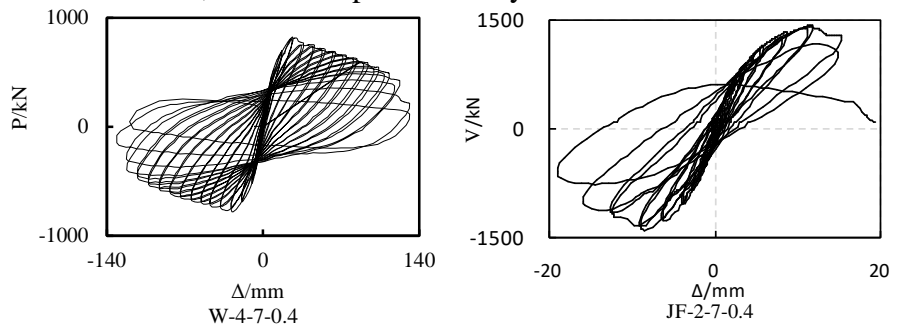


Fig.5 Load-displacement curves of specimens

Due to the axial compression of specimens is larger, there is no obvious crack point on the skeleton curve, so the yield point, peak load point and limit displacement can be considered the characteristic point of the skeleton curve. Table 2 lists the test results.

Number	Loading	Yield point		Peak load point		Limit displacement		du a4:1:4v	
	direction	P _y /kN	$\Delta_{\rm y}/{ m mm}$	P _m /kN	$\Delta_{\rm m}/{\rm mm}$	P _u /kN	$\Delta_{ m u}/{ m mm}$	ductility	
WF-4-7-0.4	positive	702.0	17.3	823.8	26.4	700.2	58.0	3.58	
	negative	658.4	17.0	780.2	28.0	663.1	64.8		
JF-2-7-0.4	positive	1220.0	6.97	1425.3	11.78	1	-	1.67	
	negative	1201.9	5 17	1417.2	8 51	_	_		

Table 2 Test results of specimens

3.3 The deformation composition of the WF-4-7-0.4

Fig.6 illustrates that the total deformation consists of bending deformation (Δf), shear

deformation (Δ s) and bonding slip deformation (Δ slip). The deformation of the yield point, peak load point and limit displacement point is calculated according to the test value in Fig.3 and the following formula, and the results are shown in table 3.

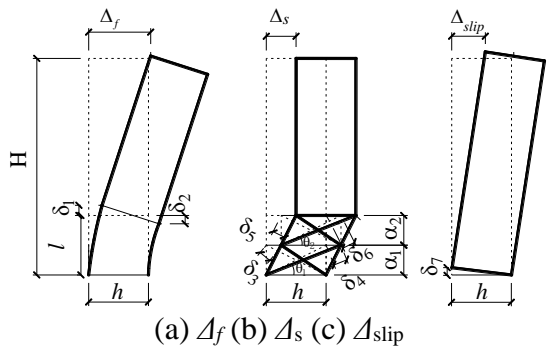


Fig.6 The three main deformation components

$$\Delta_f' = (H - 0.5l)(\delta_1 - \delta_2) / h$$
 (1)

$$\Delta_{s} = \frac{\left|\delta_{3}\right| + \left|\delta_{4}\right|}{2\cos\theta_{1}} + \frac{\left|\delta_{5}\right| + \left|\delta_{6}\right|}{2\cos\theta_{2}}$$

$$= \frac{(\left|\delta_{3}\right| + \left|\delta_{4}\right|)\sqrt{a_{1}^{2} + h^{2}}}{2h} + \frac{(\left|\delta_{5}\right| + \left|\delta_{6}\right|)\sqrt{a_{2}^{2} + h^{2}}}{2h}$$
(2)

$$\Delta_{slip} = \delta_7 H / h_0 \tag{3}$$

$$\Delta_f'' = \Delta - \Delta_f' - \Delta_s - \Delta_{slin} \tag{4}$$

Where 1 is the height of dial indicators in the plastic hinge region. $\Delta f'$ is the deformation of plastic hinge region 1. $\Delta f''$ is the bending deformation of H-1 range caused by fracture and elastic deformation. Δ is the level displacement specimens. $\delta 1 \sim \delta 7$ is the elongation or compression value of dial indicators.

In table 3, Δf is the total bending deformation of specimens, namely $\Delta f = \Delta f' + \Delta f''$. Δ' is the plastic hinge region deformation caused by bending, shear and slip deformation, namely $\Delta' = \Delta f' + \Delta s + \Delta s$ ip. It is can be seen form the table 3, the deformation $\Delta f'$ is about 70%~80% of the plastic hinge region deformation Δ' , and is about 60%~70% of the total deformation Δ . The total bending deformation Δf is about 70%~80% of the total deformation Δ . The plastic hinge region deformation Δ' is about 90% of the total deformation Δ , and the value increases as the displacement increases.

Number	Loading		Δ_f'/mm $((\Delta_f'/\Delta')/\%)$	Δ_s /mm $((\Delta_s/\Delta')/\%)$	$\Delta_{ m slip}$ /mm $((\Delta_{ m slip}$ / Δ')/%)	Δ_f "/mm $((\Delta_f$ "/ Δ)/%)	Δ_f'/Δ (%)	Δ_f/Δ (%)	Δ'/Δ (%)
WF-4- 7-0.4	Yield point	positive	21.45(84.7)	1.71(6.8)	2.17(8.6)	1.08(4.1)	81.2	85.3	95.9
		negative	22.69(84.5)	1.72(6.4)	2.43(9.1)	1.14(4.1)	81.1	85.2	95.9
	Peak load point	positive	47.47(85.7)	3.58(6.5)	4.35(7.9)	2.59(4.5)	81.9	86.3	95.5
		negative	53.22(85.9)	4.50(7.3)	4.20(6.8)	2.88(4.4)	82.1	86.6	95.6
	Limit	positive	11.23(84.0)	1.05(7.9)	1.09(8.2)	0.65(4.6)	80.1	84.7	95.4
	displacement	negative	12.25(84.5)	1.11(7.7)	1.14(7.9)	0.57(3.8)	81.3	85.1	96.2

Table 3 Test results of deformation

3.4 Energy dissipation capacity

The relationship between the Equivalent viscous damping coefficient he and the Angle θ at the

top of the column is shown in Fig.7. It can be seen from the figure 7, the early loading, equivalent viscous damping coefficient of the two specimens is approximation equal, but specimens WF - 4-7-0.4 have larger the deformation, thus which have a good energy dissipation capacity, and the viscous damping coefficient increases with the increase of angle, however, the energy dissipation capacity of specimen JF-2-7-0.4 is very poor.

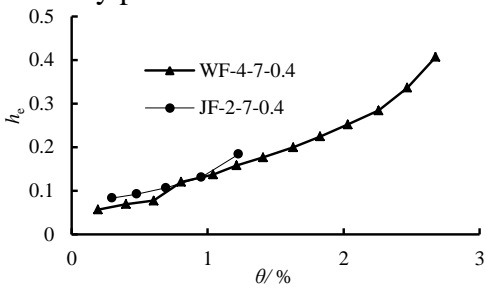


Fig.7 Equivalent viscous damping coefficient

4. Conclusions

Specimen WF-4-7-0.4 occurs bending failure, and the hysteresis curve is full, the specimen has stronger energy dissipation ability and displacement ability, and the displacement ductility coefficient is greater than 3. The displacement of WF-4-7-0.4 is mainly composed of bending deformation, shear deformation and sliding deformation of plastic hinge region, which is about 90% of the total deformation. The bending deformation is about 70%~80% of the total deformation. The specimens JF-2-7-0.4 occur shear bond failure, Its failure characteristics are that there are some vertical bond cracks in the intermediate longitudinal steel bar position of specimen, and the diagonal cracks development faster with the increase of the horizontal load, the diagonal cracks and vertical cracks intersect, so that the concrete falls off rapidly and the bearing capacity decreases sharply, and the specimen JF-2-7-0.4 has lower energy dissipation ability and displacement ability

References

[1] Y.H.ZHANG, C.K.HUANG, G.F.ZHAO: Using X-shaped reinforcing to improve anti-seismic capability of short columns. Journal of Dalian University of Technology. 38. (1998), No. 3, 332–336.

[2] GIOVANNI MINAFÒ, F. DI TRAPANI, GIUSEPPINA AMATO: Strength and ductility of RC jacketed columns: a simplified analytical method. Engineering Structures.122. (2016),184–195.

[3] KYOUNG-K.C, GIA.T.T, JONG.C.K: Seismic performance of lightly shear reinforced RC columns. Engineering Structures. 126. (2016),490–504.

[4] HABER.Z.B, SAIIDI.M.S,SANDERS.D.H: Seismic Performance of Precast Columns with Mechanically Spliced Column-Footing Connections. ACI Structural Journal. 111.(2014),No.3, 339–650.

[5] S.Q. HE, R.X.AN, L.Z.SONG: Effects of clip steel bar on failure modes of reinforced concrete columns under low cycle reversed loading. China Civil Engineering Journal. 42. (2009),No.2, 17–23.

[6] YAN X, HENRY W.Y: Experimental studies on full-scale high-strength concrete columns.ACI Structural Journal. 99. (2002),No.2,199–207.

[7] X.L.LV, G.J.ZHANG, S.L.CHEN: Research on seismic behavior of full-scale high-strength concrete frame columns with high axial compression ratios. Journal of Building Structures. 30. (2009), No.3, 20–26.

[8] Z.B.LI, J.SONG, X.L.DU, X.G.YANG: Size effect of confined concrete subjected to axial compression. Journal of Central South University. 21. (2014), 1217–1226.

[9] JAE-II SIM, K.H.YANG, KIM H.Y, CHOI B.J: Size and shape effects on compressive strength of lightweight concrete. Construction and Building Materials. 38. (2013), 854–864.

[10] S.T.YI, E.K.YANG, J.C.CHOI: Effect of specimen sizes, specimen shapes, and placement directions on compressive strength of concrete. Nuclear Engineering and Design. 236. (2006), No.2,115–127.

[11] J.R.DEL VISO, J.R. CARMONA, G. RUIZ: Shape and size effects on the compressive strength of high-strength concrete. Cement and Concrete Research. 38. (2008), No.3, 386–395.

- [12] KIM J.E, PARK W.S, EOM N.Y: Size effect on compressive strength and modulus of elasticity in high performance concrete. Advanced Materials Research. 634. (2013), No.1, 2742–2745.
- [13] Y.F.WANG, H.L.WU: Size effect of concrete short columns confined with aramid FRP jackets. Journal of Composites for Construction. 15. (2011), No.4, 535–544.
- [14] MOTAZ M.E, KRAUTHAMMER.T: Dynamic size effect in normal and high-strength concrete cylinders. ACI Materials Journal. 102. (2005), No.2, 77–85.
- [15] SHEIKH S.A, TOKLUCU M.T: Reinforced concrete columns confined by circular spiral and hoops. ACI Structure Journal. 90. (1993), 542–553.